Supplement of Geochronology, 6, 409–427, 2024
https://doi.org/10.5194/gchron-6-409-2024-supplement

Supplement of

New age constraints reveal moraine stabilization thousands of years after deposition during the last deglaciation of western New York, USA

Karlee K. Prince et al.

Correspondence to: Karlee K. Prince (karleepr@buffalo.edu)

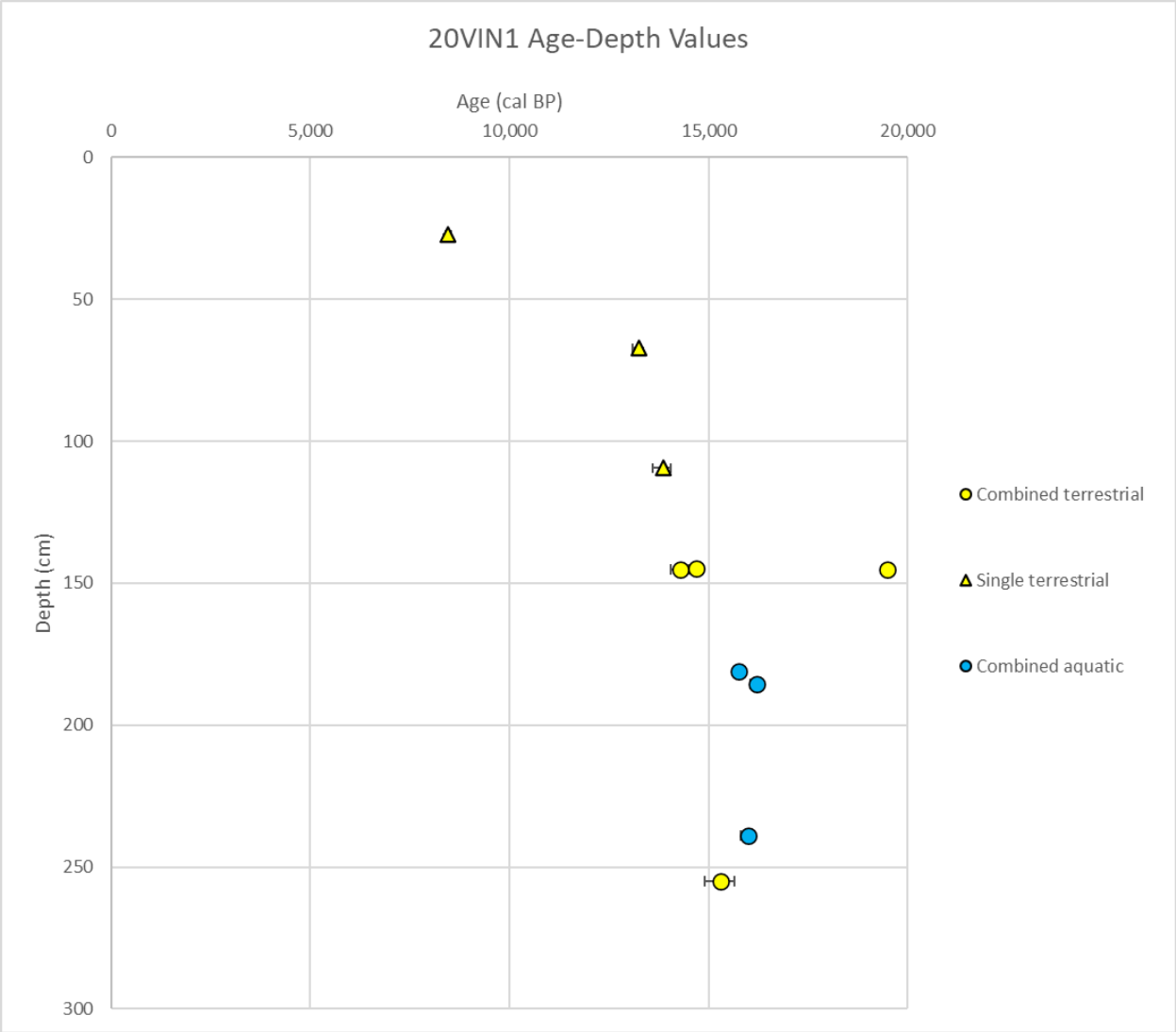

Figure S1. 20VIN1 age-depth values plotted by depth and symbolized by terrestrial vs aquatic nature and single vs combined nature. Depth begins at the top of the sediment core and for this coring location that is the surface of the bog.

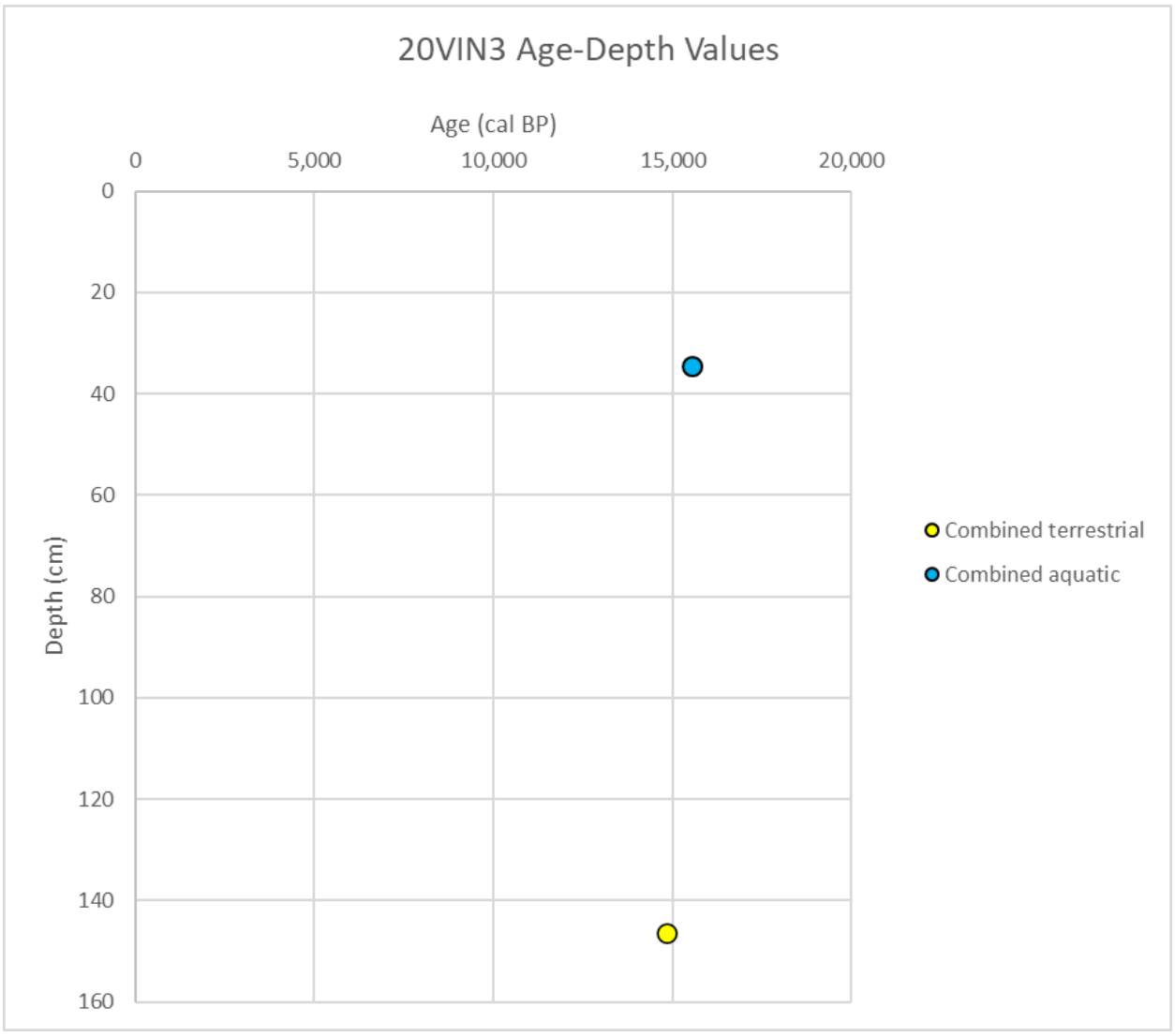

Figure S2. 20VIN3 age-depth values plotted by depth and symbolized by terrestrial vs aquatic nature and single vs combined nature. Depth begins at the top of the sediment core and for this coring location that is not the surface of the bog.

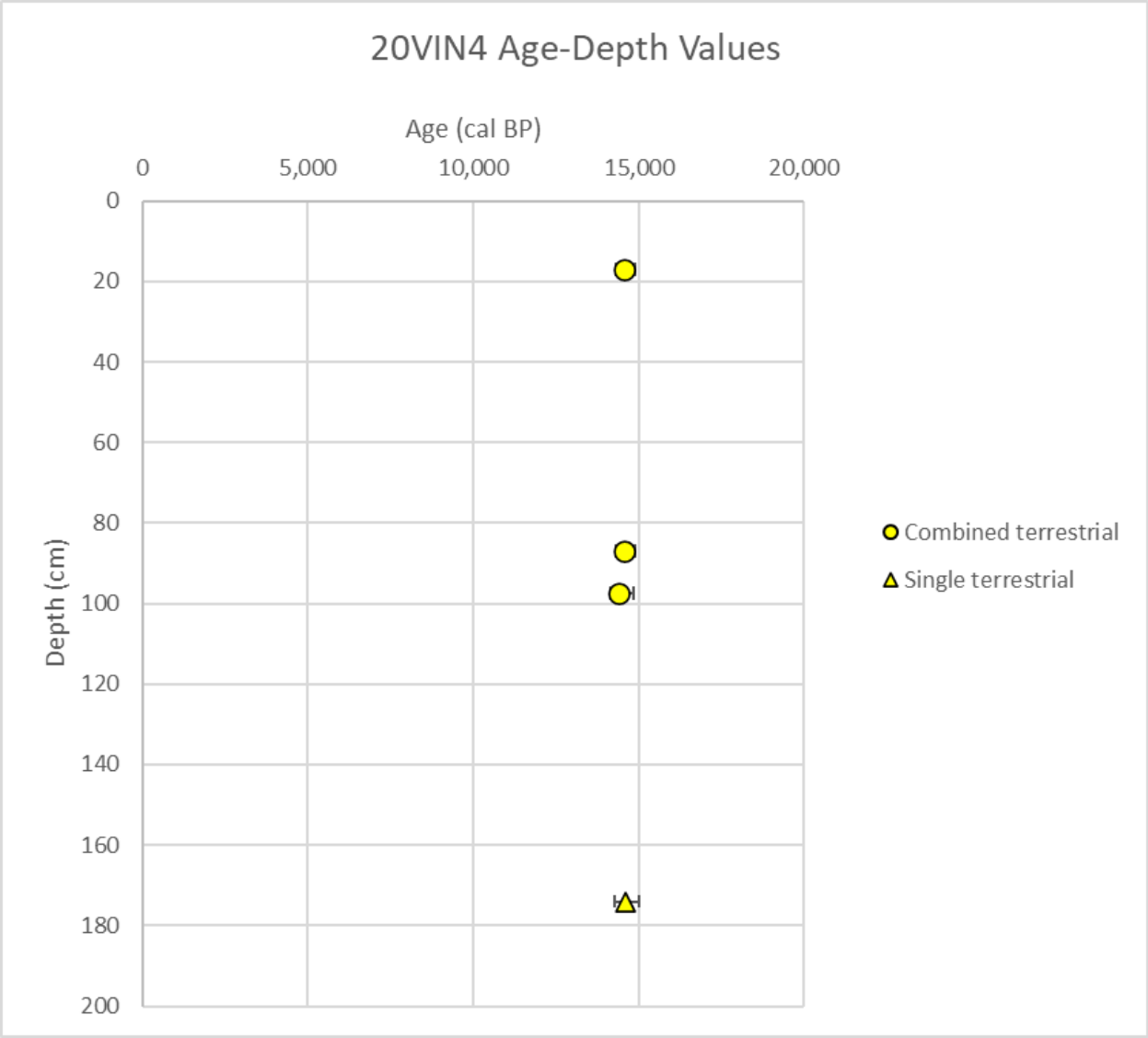

Figure S3. 20VIN4 age-depth values plotted by depth and symbolized by terrestrial vs aquatic nature and single vs combined nature. Depth begins at the top of the sediment core and for this coring location that is not the surface of the bog.

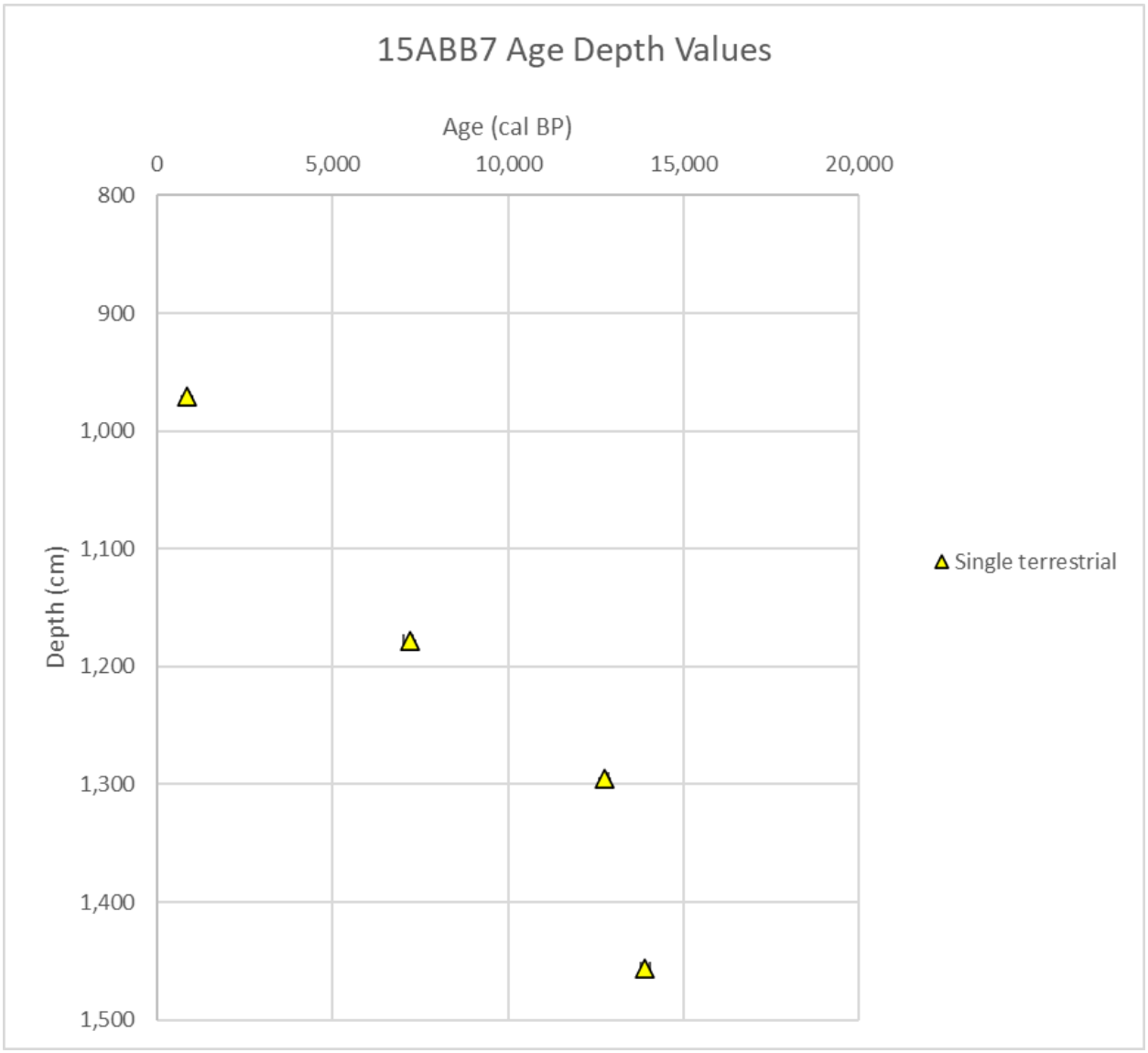

Figure S4. 15ABB7 age-depth values plotted by depth and symbolized by terrestrial vs aquatic nature and single vs combined nature. Depth begins at the top of the sediment core and for this coring location that is not the surface of the bog.

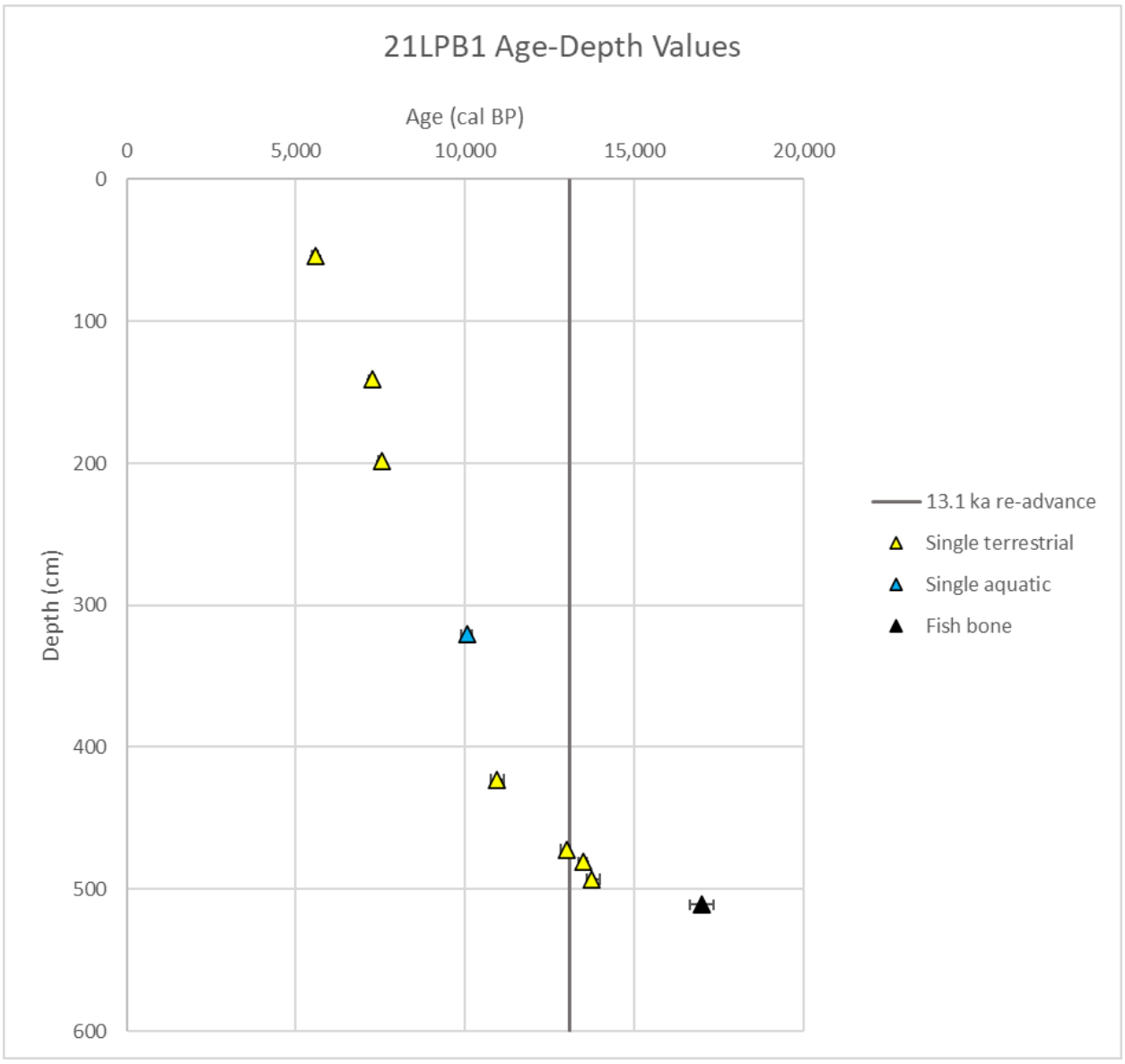

Figure S5. 21LPB1 age-depth values plotted by depth and symbolized by terrestrial vs aquatic nature and single vs combined nature. The timing of the Allerød re-advance hypothesis is shown by the gray line. Depth begins at the top of the sediment core and for this coring location that is the surface of the bog.

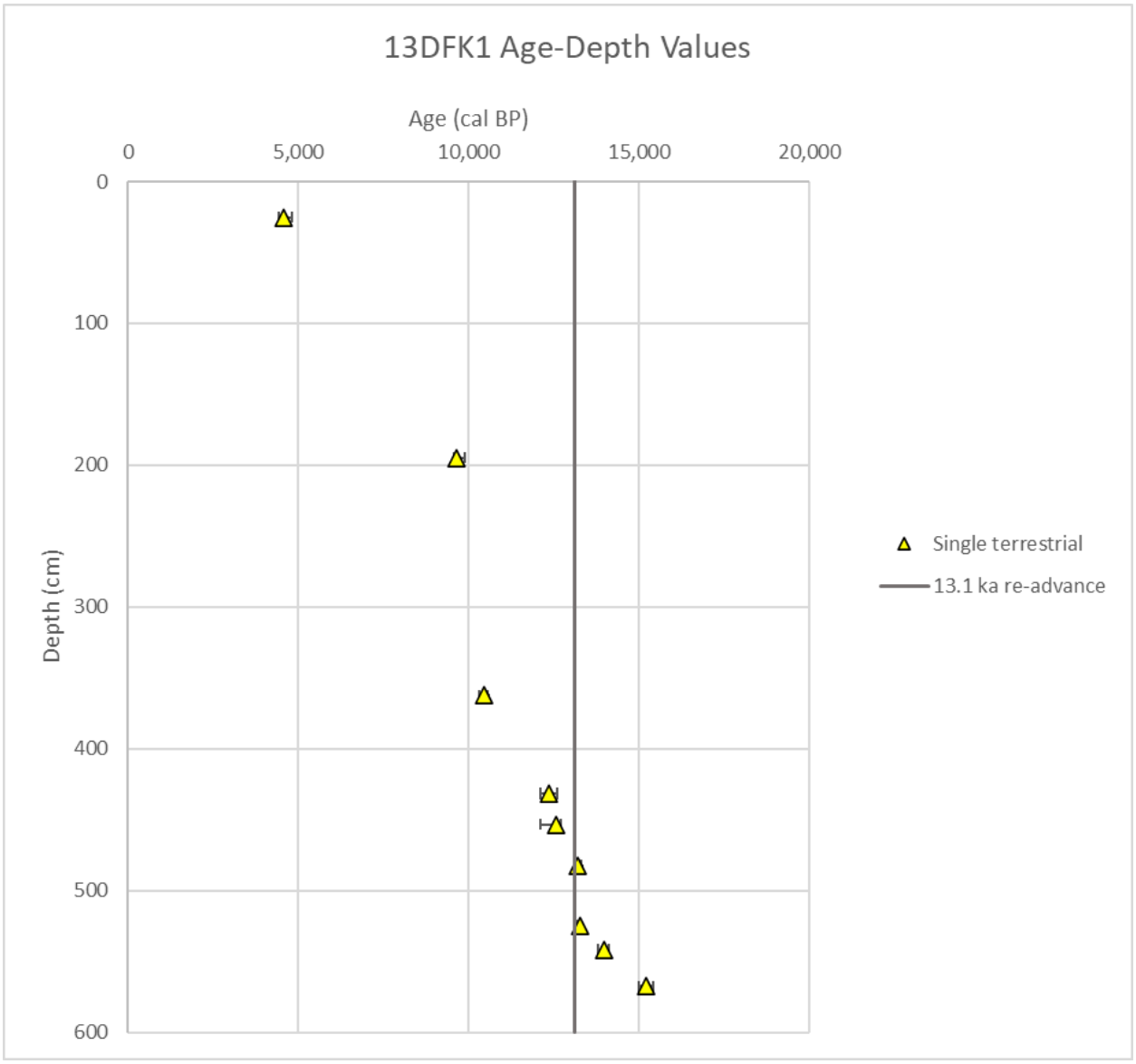

Figure S6. 13DFK1 age-depth values plotted by depth and symbolized by terrestrial vs aquatic nature and single vs combined nature. The timing of the Allerød re-advance hypothesis is shown by the gray line. Depth begins at the top of the sediment core and for this coring location that is the surface of the bog.

43

Table S1. Dose Rate Information

USU num.	Lat/Long	In-situ H_2O (%)	D_R Subsample[1]	K (%)[2]	Rb (ppm)[2]	Th (ppm)[2]	U (ppm)[2]	Cosmic (Gy/kyr)
USU-3622	42.11394/ -78.94899	7.5	F: 70%	1.64±0.04	77.6±3.1	7.8±0.7	2.6±0.2	0.18±0.02
			M: 20%	1.12±0.03	58.7±2.3	8.6±0.8	2.2±0.2	
			C: 10%	1.29±0.03	76.1±3.0	11.1±1.0	2.1±0.1	
USU-3623	42.11394/ -78.94899	20.0	F: 85%	1.52±0.04	74.4±3.0	8.3±0.7	2.0±0.1	0.18±0.02
			M: 15%	1.35±0.03	72.7±2.9	8.4±0.8	2.4±0.2	

[1] Dose rate (D_R) subsamples based on grain size: fine-F (<1.7 mm), medium-M (1.7-16 mm), coarse-C (>16 mm), and weighted proportions (%) of subsamples used with chemistry in gamma dose rate calculation. Beta dose rate uses chemistry from fine fraction (<1.7 mm) only.

[2] Radioelemental concentrations determined using ICP-MS and ICP-AES techniques; dose rate is derived from concentrations by conversion factors from Guérin et al. (2011).

44

45

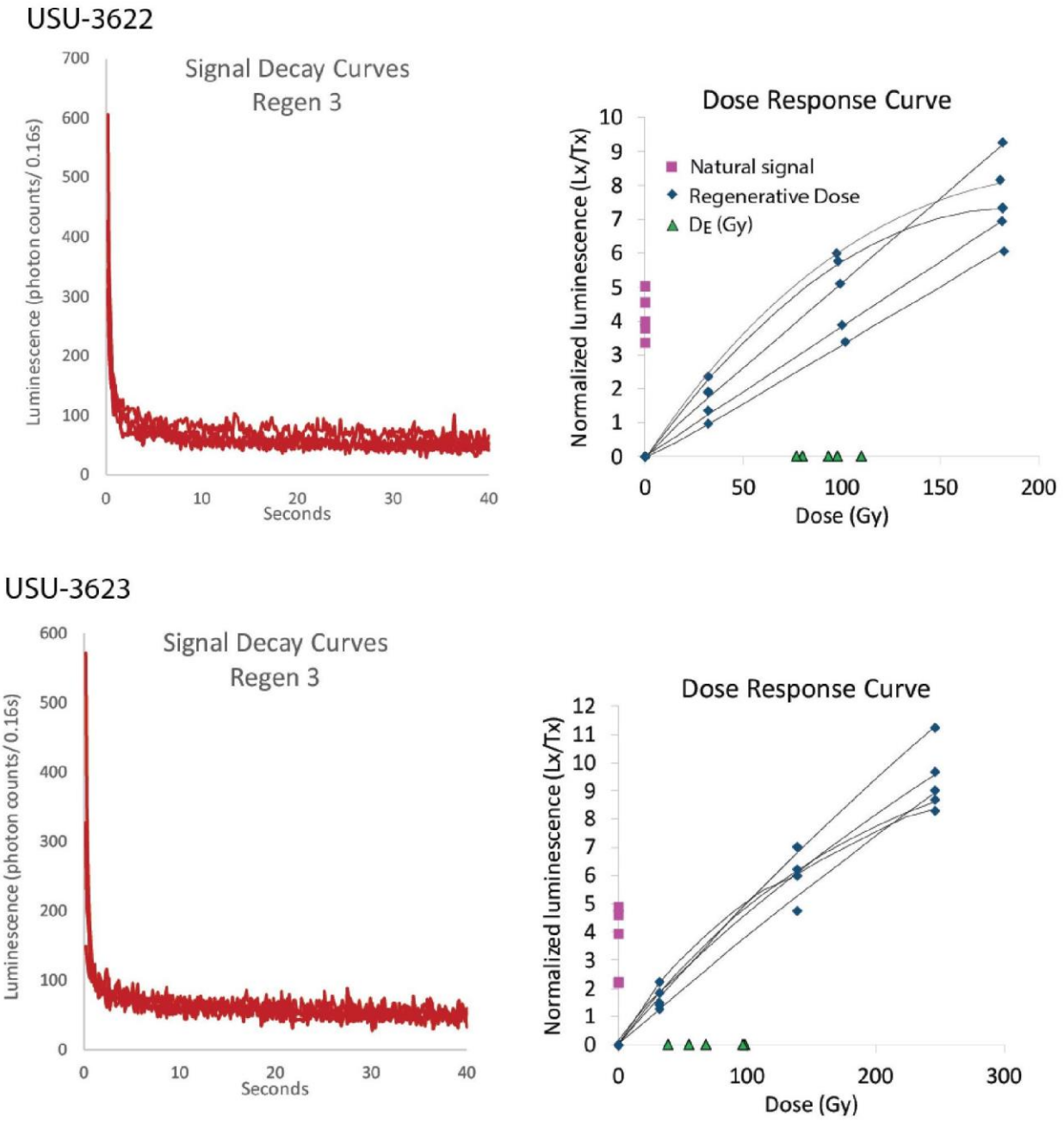

Figure S7. Example luminescence signal decay (left) and dose-response curves from 5 aliquots from each of the luminescence samples.